Physica B 405 (2010) 2423–2426

Contents lists available at ScienceDirect

Physica B

journal homepage: www.elsevier.com/locate/physb

Effect of doping on the Raman scattering of 6H-SiC crystals

Xiang-Biao Li*, Zhi-Zhan Chen, Er-Wei Shi

Shanghai Institute of Ceramics, Chinese Academy of Sciences, Shanghai 200050, China

ARTICLE INFO

Article history:
Received 7 November 2009
Received in revised form
23 February 2010
Accepted 25 February 2010

Keywords:
Raman scattering
Silicon carbide crystal
Doping

ABSTRACT

Raman spectra of Al- and N-doped 6 H-SiC crystal samples with different doping levels were measured. The first-order Raman spectra of the samples were shifted to higher frequency when the doping concentrations were increased. Compared with Al-doped samples, the intensity of A_1 longitudinal optical mode of N-doped ones changed obviously, which reflected the different doping concentrations. The second-order Raman spectra were not dependent on the doping types and concentrations.

1. Introduction

Silicon carbide (SiC) crystals have recently been recognized as an important material for a wide variety of high-power, high-frequency and high-temperature electronic applications. As a perfect wide band gap semiconductor, SiC is an insulator up to high temperatures. Incorporation of foreign dopants can create states relatively close to the conduction or valence band edges, which allows excitation of electron (donor) or hole (acceptor) into the bands. Characterization of doped SiC is essential for the development of SiC materials and devices. N- or p-type carriers can be achieved by doping different ions, and the conductivity is proportional to the doping concentration. The shallower the dopant states, the lower the temperature where the full dopant concentration becomes active. Nitrogen (N) or phosphorus (P) for n-type, aluminum (Al) or boron (B) for p-type and vanadium (V) for semi-insulating type, are often chosen for SiC doping.

Raman scattering measurement is a powerful technique for the characterization of SiC, because it is non-destructive and requires no special preparation of samples. The Raman efficiency of SiC is high because of strong covalency of the bonding and the Raman signals are easily obtained. Raman scattering has been practically used for the evaluation of structural and electrical properties of SiC crystals. The Raman parameters such as intensity, width, peak frequency shift and polarization of Raman bands provide valuable information on the crystal quality [1–3]. Raman analyses of the stacking structure of polytypes, stacking disorder, strain, polytype conversion and damage in ion-implanted SiC were widely investigated [4–7]. Another advantage of Raman scattering is the capability of characterization of electronic properties in polar semiconductors. Raman measurements enable detection of coupled modes of LO phonon and plasma oscillation of free carriers whose spectral features depend on the carrier concentration and carrier damping. Therefore, the Raman spectroscopic technique will be widely used to evaluate SiC crystals in the near future because of its usefulness.

Nitrogen is well established as a donor in SiC. Significant changes were observed in the shape and position of the A_1 longitudinal optical (LO) phonon as a function of doping concentration. The changes in peak position, spectral shape and width of the A_1(LO) phonon are attributed to plasmon–phonon coupling. Unlike nitrogen doping, the effect of aluminum doping on Raman scattering was rarely reported. The peak frequency shift mechanism after N and Al doping was not investigated systematically. In this work, we have performed Raman scattering measurements on Al-, lower and heavily N-doped 6H-SiC crystals at room temperature. Second-order Raman spectra of 4H-, 6H- and 15R-SiC are also presented. The first-order Raman spectra of SiC are polytype dependent mainly due to the existence of the folded modes. Changes of the Raman frequency and intensity of the peaks are studied. The Raman peaks of Al- and N-doped 6H-SiC shift to high frequency. The peak frequency shift mechanisms are put forward.

2. Experiment

SiC single crystals were grown in a conventional physical vapor transport (PVT) setup [8]. Nitrogen doping was performed by mixing nitrogen gas to the argon growth atmosphere. Aluminum

* Corresponding author. Tel.: +86 21 52411109.
E-mail address: xiangbiao_li@yahoo.com.cn (X.-B. Li).

0921-4526/$ - see front matter © 2010 Elsevier B.V. All rights reserved.
doi:10.1016/j.physb.2010.02.058

doping was achieved by mixing aluminum carbide (Al_4C_3) to the high-purity SiC powder.

The Raman spectra were measured by JOBLN-YVON T64000 Raman spectrometer at room temperature using the 514.5 Å line of an argon ion laser as the excitation source. The carrier concentration was measured by the van der Pauw method on a Hall effect measurement system (LakeShore, EM4 Series and EM7 Electromagnets system). The glow discharge mass spectrometer (GDMS) analysis system (VG9000, Thermo Elemental) was chosen to measure the Al content. The Al content was 52 ppm (wt%).

3. Results and discussion

6H-SiC has a wurtzitic structure with C_{6v}^4 space group. The Raman active modes are of A_1, E_1 and E_2 symmetry. Since optical branches of A_1 and E_1 symmetry phonon modes are both Raman and IR active, they split into longitudinal and transverse branches. Fig. 1 shows the first-order Raman spectra of undoped and Al-doped 6H-SiC samples. For undoped SiC sample, four Raman peaks were observed; they were E_2 planar optical (PO) peaks at 765 cm^{-1} (x=1), 787 cm^{-1} (x=0.33), E_1 transverse optical (TO) peak at 795 cm^{-1} and A_1 longitudinal optical (LO) peak at 964 cm^{-1}. As for the Al-doped sample, all the Raman peaks shifted by about 1 cm^{-1} to higher frequency. The effect of N doping concentration on the first-order Raman spectra is illustrated in Fig. 2, and the Raman peak identification is listed in Table 1. One the one hand, the symmetry and intensity of A_1 (LO) mode of N-doped samples decreased sharply with increasing N doping concentrations. One the other hand, the Raman peaks of N-doped samples also shifted to high frequency, similar to Al-doped ones. However, the effect of carrier concentration on Raman shift is obvious, especially for the A_1 mode. For example, the carrier concentration of undoped sample is as low as 4.6×10^{15} cm^{-3}; the Raman peak of A_1 mode was at 964 cm^{-1}. When the carrier concentration was increased to 5.1×10^{18} cm^{-3} for high N-doped sample, the corresponding Raman peak of A_1 mode was shifted by almost 4 cm^{-1}.

The LO phonon–plasmon coupled mode is often chosen to analyze the A_1 (LO) mode[11]. This mode consists of three components such as deformation potential, electro-optical and charge-density fluctuation. SiC has a large band gap and low carrier mobility, which means that the electro-optical and deformation potential mechanisms dominate the scattering. The spectral shape depends on the amount of plasmon damping due to carrier scattering. The line shape of the LO phonon can be

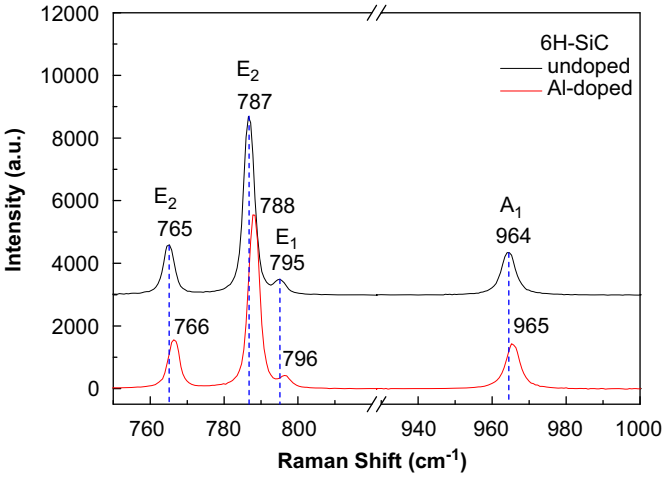

Fig. 1. First-order Raman spectra of undoped and Al-doped 6H-SiC samples.

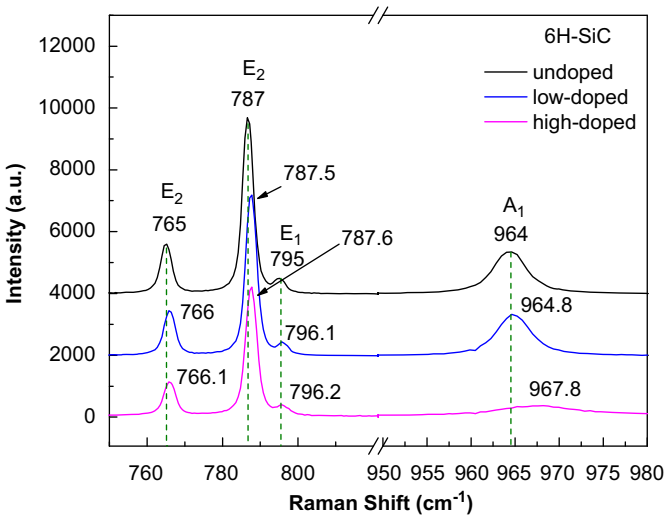

Fig. 2. First-order Raman spectra of undoped, low N-doped and high N-doped 6H-SiC samples.

Table 1
Carrier concentration and Raman shifts for different N-doped 6H-SiC samples.

Sample	Undoped	Low N-doped	High N-doped
Carrier concentration (cm^{-3})	4.6×10^{15}	2.4×10^{16}	5.1×10^{18}
Peak Raman shift (cm^{-1})			
E_2 (PO)	765.0	766.0	766.1
E_2 (PO)	787.0	787.5	787.6
E_1 (TO)	795.0	796.1	796.2
A_1 (LO)	964.0	964.8	967.8

described by [11–13]

$$I(\omega)=SA(\omega)\mathrm{Im}\left[-\frac{1}{\varepsilon(\omega)}\right] \tag{1}$$

where S is a proportionality constant, ω is the Raman shift, $\varepsilon(\omega)$ the dielectric function and $A(\omega)$ is given by

$$A(\omega)=1+\frac{2C\omega_T^2[\omega_P^2\gamma(\omega_T^2-\omega^2)-\omega^2\Gamma(\omega^2-\gamma^2-\omega_P^2)]}{\Delta}+\left(\frac{C^2\omega_T^2}{\Delta}\right)\left(\frac{\omega_P^2[\gamma(\omega_L^2-\omega_T^2)+\Gamma(\omega_P^2-2\omega^2)]+\omega^2\Gamma(\omega^{2+}\gamma^2)}{(\omega_L^2-\omega_T^2)}\right) \tag{2}$$

Here, ω_L and ω_T are the longitudinal and transverse optical phonon frequencies, respectively, γ is the plasmon dampening constant, Γ the phonon dampening constant, $\Delta=\omega_p^2\gamma\left[(\omega_T^2-\omega^2)^2+(\omega\Gamma)^2\right]+\omega^2\Gamma(\omega_L^2-\omega_T^2)(\omega^2+\gamma^2)$, C is the Faust–Henry coefficient and

$$\varepsilon(\omega)=\varepsilon_\infty\left(1+\frac{\omega_L^2-\omega_T^2}{\omega_T^2-\omega^2-i\omega\Gamma}-\frac{\omega_P^2}{\omega(\omega+i\gamma)}\right)$$

contains a phonon and a plasmon contribution. The plasma frequency$\omega_P=\left((ne^2 4\pi)/(m_{eff}\omega_\infty)\right)^{1/2}=c(n)^{1/2}$, in which $c=\left((4e^2\pi)/(m_{eff}\omega_\infty)\right)^{1/2}$is related to optical dielectric constant (ε_∞), electron effective mass (m_{eff}) and doping concentration (n). The value of ω_P increased when the doping concentration (n) increased, enhancing the coupling interaction between phonons and plasmon. Consequently, the A_1 (LO) phonon frequency increased and shifted to higher wavenumber when the carrier concentration was increased. On the other hand, increasing ω_P induced the dampening of phonon enlargement. The intensity of

A_1 (LO) became lower and the full-width at half-maximum was broadened (Fig. 2).

The mechanisms of Raman shift of Al- and N-doped samples are different. The influence of Al doping on the Raman shift was mainly contributed to the atomic size effect. When Al atoms are doped in SiC, they always occupy Si lattice positions. The size effect is expected to result in an increase of the lattice parameter due to the bigger radius of Al. The interatomic distances of Si–C bond and Al–C bond are 1.89 and 1.97 Å, respectively. The biaxial compressive stress will be released gradually. It results in an increase of the phonon oscillation frequency. The Raman peaks shift to high frequencies. Doping Al and N causes import of holes (acceptors) and carriers (donor), respectively. The carriers are more active than the holes at room temperature. The hole mobility is dependent on the temperature, doping and anisotropy of the crystal structure [14]. The interaction between the carriers and the phonons is more effective than that between the holes and phonons. Although the N-doped samples also have the atomic effect, effect of high carrier concentration is predominant, the atomic effect is not considered.

The first-order Raman spectra are sensitive only to phonons at the Γ point ($k=0$) of the first Brillouin zone, due to the need to conserve crystal momentum. Second-order Raman spectra give information about the entire Brillouin zone because the modes are due to the combination of two phonons. As for the second-order Raman spectra, two wave vectors have a combined wave vector where k is close to zero. The selection rules are more difficult to satisfy. The most important reason for this is that momentum conservation involves two phonons so that the scattering process need not originate near the Brillouin zone center as in the first-order effect.

The second-order Raman spectra of undoped, Al- and N-doped 6H-SiC samples are shown in Fig. 3. The Raman peaks are marked as a (1477 cm^{-1}), b (1514 cm^{-1}), c (1530 cm^{-1}), d (1543 cm^{-1}), e (1580 cm^{-1}), f (1618 cm^{-1}), g (1651 cm^{-1}), h (1683 cm^{-1}), i (1712 cm^{-1}) and j (1928 cm^{-1}). The optical branch of the overtone or combined phonons spectra has been observed to begin at 1477 cm^{-1} for all samples. There are no phonons that are capable of being doubled to frequencies of just less than 1477 cm^{-1}, which can be verified in Figs. 1 and 2. The lowest point in the second-order Raman spectra is the K point phonon dispersion curve. It was calculated by Hofmann et al. [9] and measured by Patrick et al. [10] for 2H-SiC as 737 cm^{-1}. Considering the frequency of the K point phonon of 6H-SiC similar to that of 2H-SiC, the 1477 cm^{-1} is due to the overtone of the K point phonon. The highest point is approximately at j (1928 cm^{-1}) due to the overtone of the Γ point A_1 (LO) phonon at 964 cm^{-1}. There are several peaks in the range b–e. The b point is consistent with an overtone of the L point phonon and d is due to the overtone of M point phonon TO_1 mode. The additional peak c is possibly due to a phonon from another point on the L–M branch, such as the 765 cm^{-1} mode at the U point. The L–M branch dispersion curves are clearly shown in calculations [9]. The peak h is due to the overtone of M point phonon TO_2 mode. According to the result of Burton et al. [4], the broader peak i is due to the overtone of the M point phonon at 857 cm^{-1}. Theoretical calculation showed that a gap exists in the phonon density of states approximately between 785 and 840 cm^{-1} [9]. The e, f and g modes are less intensive and due to combinations of phonons from different branches, not from the optical overtones. It is observed that all the peaks of doped samples are the same as those of undoped ones. No peaks stemmed from the local mode vibrations of Al acceptors or N donors due to the absence of a scaling effect. The conductivity types and doping concentrations have no influence on the second-order Raman scattering of SiC crystals [4].

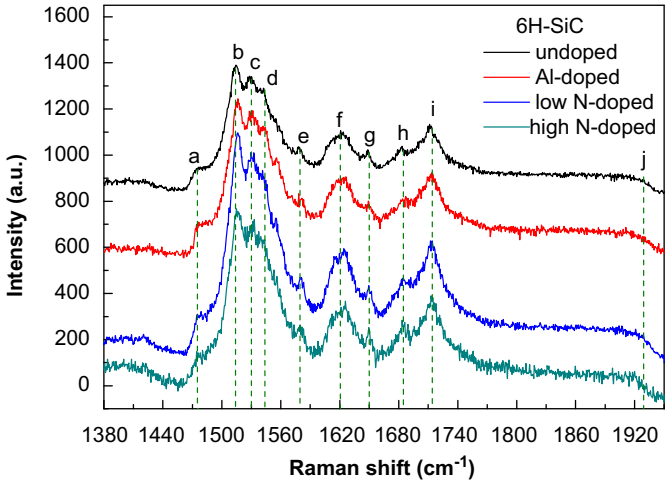

Fig. 3. Second-order Raman spectra of undoped, Al- and N-doped 6H-SiC samples.

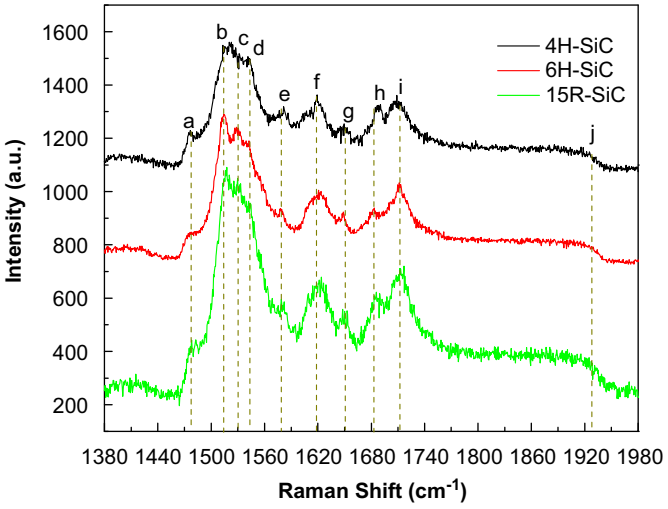

Fig. 4. Second-order Raman spectra of 4H-, 6H- and 15R-SiC samples.

The second-order Raman scattering is also independent of polytypes, such as 4H-, 6H- and 15R-SiC crystals as shown in Fig. 4. The three polytypes had unanimous second-order Raman peaks positions and are consistent with those of the doped samples. No Raman shifts were observed. In fact, since the density of double-phonon states tends to become greater for larger phonon wave vectors, it is likely that the observed second-order scattering originates near the Brillouin zone boundary. Therefore double-layer structures of SiC polytypes, such as 4H-, 6H- and 15R-SiC, have similar second-order Raman spectra.

4. Conclusion

In summary, the first-order Raman spectra of SiC are polytype dependent mainly due to the existence of the folded modes. The Raman frequency and intensity of the peaks depend on the polytype and doping concentrations. Although the Raman peaks of Al- and N-doped 6H-SiC shift to high frequency, the shift mechanisms are different. The former is due to the size effect and the latter is due to the coupling of the LO phonon to overdamped plasmons. The second-order Raman spectra are independent of polytype, conductivity and doping type.

Acknowledgements

This work was supported by "863" Project (2006AA03A146), Knowledge Innovation Program of the Chinese Academy of Sciences (KGCX2-YW-206), Natural Science Foundation of Shanghai (06ZR14096) and Science and Technology Commission of Shanghai Municipality (09DZ1141400, 09520714900).

References

[1] Ma Jian-ping, Chen Zhi-ming, Lu Gang, Hang Lian-mao, Feng Xian-feng, Lei Tian-min, Chin. Phys. Lett. 18 (2001) 1123.
[2] You Jing-Lin, Jiang Guo-Chang, Hou Huai-Yu, Wu Yong-Quan, Chen Hui, Xu Kuang-Di, Chin. Phys. Lett. 19 (2002) 205.
[3] Li Chao-Rong, Wu Li-Jun, Chen Wan-Chun, Chin. Phys. Lett. 19 (2002) 714.
[4] J.C. Burton, L. Sun, F.H. Long, Z.C. Feng, I.T. Ferguson, Phys. Rev. B 59 (1999) 7282.
[5] S. Nakashima, K. Kisoda, J.-P. Gauthier, J. Appl. Phys. 75 (1994) 5354.
[6] S. Nakashima, H. Harima, Phys. Status Solidi A 162 (1997) 39.
[7] S. Nakashima, H. Katahama, Y. Nakaura, A. Mitsuishi, Phys. Rev. B 33 (1986) 5721.
[8] Li Xiang-Biao, Shi Er-Wei, Chen Zhi-Zhan, Xiao Bing, Diamond Relat. Mater. 16 (2007) 654.
[9] M. Hofmann, A. Zywietz, K. Karch, F. Bechstedt, Phys. Rev. B 50 (1994) 13401.
[10] Lyle Patrick, D.R. Hamilton, W.J. Choyke, Phys. Rev. 143 (1966) 526.
[11] M.V. Klein, B.N. Gsnguly, P.J. Colwell, Phys. Rev. B 6 (1972) 2380.
[12] Hiroshi Harima, Shin-ichi Nakashima, Tomoki Uemura, J. Appl. Phys. 78 (1995) 1996.
[13] J.C. Burton, L. Sun, M. Pophristic, S.J. Lukacs, F.H. Long, Z.C. Feng, I.T. Ferguson, J. Appl. Phys. 84 (1998) 6268.
[14] A. Martinez, U. Lindefelt, M. Hjelm, H.-E. Nilsson, Appl. Surf. Sci. 184 (2001) 173.